

Synchronized self-mode-locked 1061-nm and 1064-nm monolithic Nd:YAG laser at cryogenic temperatures with two orthogonally polarized emissions: generation of 670 GHz beating

T. L. HUANG,¹ C. L. SUNG,¹ H. P. CHENG,¹ C. Y. CHO,¹ H. C. LIANG,² K. W. SU,¹ K. F. HUANG,¹ AND Y. F. CHEN^{1,*}

¹Department of Electrophysics, National Chiao Tung University, Hsinchu, Taiwan

²Institute of Optoelectronic Science, National Taiwan Ocean University, Keelung, Taiwan

*yfchen@cc.nctu.edu.tw

Abstract: A dual-wavelength self-mode-locked monolithic Nd:YAG laser at 1061 and 1064 nm is realized at cryogenic temperatures. At an incident pump power of 5.5 W, the total output power can reach 2.5 W and the mode-locked pulse width is 29 ps at a pulse repetition rate of 7.75 GHz. The synchronization of the dual-wavelength emissions leads to a beat frequency of 670 GHz in the individual mode-locked pulse. It is further discovered that the laser output consists of two orthogonally polarized components with a central frequency difference of 127 MHz. The central frequency difference between two orthogonal polarizations mainly arises from the external mechanical stress introduced by the copper holder for the laser crystal.

©2016 Optical Society of America

OCIS codes: (140.3480) Lasers, diode-pumped; (140.3530) Lasers, neodymium; (140.3580) Lasers, solid-state; (140.4050) Mode-locked lasers.

References and Links

- G. Q. Xie, D. Y. Tang, H. Luo, H. J. Zhang, H. H. Yu, J. Y. Wang, X. T. Tao, M. H. Jiang, and L. J. Qian, "Dual-wavelength synchronously mode-locked Nd:CNGG laser," *Opt. Lett.* **33**(16), 1872–1874 (2008).
- A. Agnesi, F. Pirzio, G. Reali, A. Arcangeli, M. Tonelli, Z. Jia, and X. Tao, "Multi-wavelength diode-pumped Nd:LGGG picosecond laser," *Appl. Phys. B* **99**(1), 135–140 (2010).
- Z. Cong, D. Tang, W. De Tan, J. Zhang, C. Xu, D. Luo, X. Xu, D. Li, J. Xu, X. Zhang, and Q. Wang, "Dual-wavelength passively mode-locked Nd:LuYSiO₅ laser with SESAM," *Opt. Express* **19**(5), 3984–3989 (2011).
- Q. Yang, Y. G. Wang, D. H. Liu, J. Liu, L. H. Zheng, L. B. Su, and J. Xu, "Dual-wavelength mode-locked Nd:LuYSiO₅ laser with a double-walled carbon nanotube saturable absorber," *Laser Phys. Lett.* **9**(2), 135–140 (2012).
- Y. J. Huang, Y. S. Tzeng, C. Y. Tang, S. Y. Chiang, H. C. Liang, and Y. F. Chen, "Efficient high-power terahertz beating in a dual-wavelength synchronously mode-locked laser with dual gain media," *Opt. Lett.* **39**(6), 1477–1480 (2014).
- Y. J. Huang, H. H. Cho, Y. S. Tzeng, H. C. Liang, K. W. Su, and Y. F. Chen, "Efficient dual-wavelength diode-end-pumped laser with a diffusion-bonded Nd:YVO₄/Nd:GdVO₄ crystal," *Opt. Mater. Express* **5**(10), 2136–2141 (2015).
- M. Koch, "Terahertz technology: A land to be discovered," *Opt. Photonics News* **18**(3), 20–25 (2007).
- H. Zhong, A. Redo-Sanchez, and X. C. Zhang, "Identification and classification of chemicals using terahertz reflective spectroscopic focal-plane imaging system," *Opt. Express* **14**(20), 9130–9141 (2006).
- Y. C. Shen, T. Lo, P. F. Taday, B. E. Cole, W. R. Tribe, and M. C. Kemp, "Detection and identification of explosives using terahertz pulsed spectroscopic imaging," *Appl. Phys. Lett.* **86**(24), 241116 (2005).
- E. Pickwell and V. P. Wallace, "Biomedical applications of terahertz technology," *J. Phys. D Appl. Phys.* **39**(17), R301–R310 (2006).
- G. Q. Xie, D. Y. Tang, L. M. Zhao, L. J. Qian, and K. Ueda, "High-power self-mode-locked Yb:Y₂O₃ ceramic laser," *Opt. Lett.* **32**(18), 2741–2743 (2007).
- H. C. Liang, R. C. C. Chen, Y. J. Huang, K. W. Su, and Y. F. Chen, "Compact efficient multi-GHz Kerr-lens mode-locked diode-pumped Nd:YVO₄ laser," *Opt. Express* **16**(25), 21149–21154 (2008).
- H. C. Liang, H. L. Chang, W. C. Huang, K. W. Su, Y. F. Chen, and Y. T. Chen, "Self-mode-locked Nd:GdVO₄ laser with multi-GHz oscillations: manifestation of third-order nonlinearity," *Appl. Phys. B* **97**(2), 451–455 (2009).

14. M. T. Chang, H. C. Liang, K. W. Su, and Y. F. Chen, "Dual-comb self-mode-locked monolithic Yb:KGW laser with orthogonal polarizations," *Opt. Express* **23**(8), 10111–10116 (2015).
15. C. L. Sung, H. P. Cheng, C. Y. Lee, C. Y. Cho, H. C. Liang, and Y. F. Chen, "Generation of orthogonally polarized self-mode-locked Nd:YAG lasers with tunable beat frequencies from the thermally induced birefringence," *Opt. Lett.* **41**(8), 1781–1784 (2016).
16. F. Krausz, T. Brabec, and C. Spielmann, "Self-starting passive mode locking," *Opt. Lett.* **16**(4), 235–237 (1991).
17. C. Y. Cho, P. H. Tuan, Y. T. Yu, K. F. Huang, and Y. F. Chen, "A cryogenically cooled Nd:YAG monolithic laser for efficient dual-wavelength operation at 1061 and 1064 nm," *Laser Phys. Lett.* **10**(4), 045806 (2013).
18. W. Koehner and D. K. Rice, "Effect of birefringence on the performance of the linearly polarized YAG:Nd lasers," *IEEE J. Quantum Electron.* **6**(9), 557–566 (1970).
19. A. Owyong and P. Esherick, "Stress-induced tuning of a diode-laser-excited monolithic Nd:YAG laser," *Opt. Lett.* **12**(12), 999–1001 (1987).
20. W. Holzapfel and W. Settgest, "Force to frequency conversion by intracavity photoelastic modulation," *Appl. Opt.* **28**(21), 4585–4594 (1989).
21. S. T. Cundiff, B. C. Collings, N. N. Akhmediev, J. M. Soto-Crespo, K. Bergman, and W. H. Knox, "Observation of polarization-locked vector solitons in an optical fiber," *Phys. Rev. Lett.* **82**(20), 3988–3991 (1999).
22. J. Javaloyes, J. Mulet, and S. Balle, "Passive mode locking of lasers by crossed-polarization gain modulation," *Phys. Rev. Lett.* **97**(16), 163902 (2006).
23. S. V. Sergeev, C. Mou, A. Rozhin, and S. K. Turitsyn, "Vector solitons with locked and precessing states of polarization," *Opt. Express* **20**(24), 27434–27440 (2012).
24. J. Thévenin, M. Vallet, and M. Brunel, "Dual-polarization mode-locked Nd:YAG laser," *Opt. Lett.* **37**(14), 2859–2861 (2012).
25. M. Spanner, K. M. Davitt, and M. Y. Ivanov, "Stability of angular confinement and rotational acceleration of a diatomic molecule in an optical centrifuge," *J. Chem. Phys.* **115**(18), 8403–8410 (2001).
26. L. Tong, V. D. Miljković, and M. Käll, "Alignment, rotation, and spinning of single plasmonic nanoparticles and nanowires using polarization dependent optical forces," *Nano Lett.* **10**(1), 268–273 (2010).
27. G. D. VanWiggeren and R. Roy, "Communication with dynamically fluctuating states of light polarization," *Phys. Rev. Lett.* **88**(9), 097903 (2002).
28. N. Kanda, T. Higuchi, H. Shimizu, K. Konishi, K. Yoshioka, and M. Kuwata-Gonokami, "The vectorial control of magnetization by light," *Nat. Commun.* **2**, 362 (2011).
29. S. Sergey, C. Mou, E. Turitsyna, A. Rozhin, S. Turitsyn, and K. Blow, "Spiral attractor created by vector solitons," *Light Sci. Appl.* **3**(1), e131 (2014).
30. Y. F. Chen, Y. J. Huang, P. Y. Chiang, Y. C. Lin, and H. C. Liang, "Controlling number of lasing modes for designing short-cavity self-mode-locked Nd-doped vanadate lasers," *Appl. Phys. B* **103**(4), 841–846 (2011).
31. C. L. Wang and C. L. Pan, "Tunable multiterahertz beat signal generation from a two-wavelength laser-diode array," *Opt. Lett.* **20**(11), 1292–1294 (1995).
32. G. K. White, "Thermal expansion of reference materials: copper, silica and silicon," *J. Phys. D Appl. Phys.* **6**(17), 2070–2078 (1973).
33. R. Wynne, J. L. Daneu, and T. Y. Fan, "Thermal coefficients of the expansion and refractive index in YAG," *Appl. Opt.* **38**(15), 3282–3284 (1999).

1. Introduction

Simultaneous dual-wavelength mode-locked lasers [1–6] are of great interest for many important applications. One desirable application is the generation of coherent terahertz (THz) radiation by difference frequency generation due to its multiple applications including communications, sensing, imaging system, spectroscopic study, and material characterization [7–10]. In the past few years, the combination of the Kerr lens and thermal lensing effects has been successfully exploited to fulfill the self-mode-locked operation in various diode-end-pumped laser systems with short linear cavities [5, 6, 11–15]. It was theoretically shown [16] that the threshold intensity for self-started mode-locking at a fixed nonlinearity is proportional to the cavity round-trip time. Experimental results clearly confirm that a short cavity length is of benefit to the formation of self-mode-locking [16]. Recently, it has been found that the Nd:YAG laser can be operated at cryogenic temperatures to obtain the dual-wavelength emissions at 1061 and 1064 nm [17]. More precisely, the dominant lasing peak shifted from the wavelength of 1064 nm to the wavelength of 1061 nm at low temperatures [17]. Nevertheless, the simultaneous mode locking for the Nd:YAG 1061-nm and 1064-nm emissions have not been demonstrated so far.

On the other hand, it has been found [18–20] that the external stress can give rise to the frequency splitting for each lasing mode in the Nd:YAG laser to form the so-called two orthogonally polarized components. The orthogonally polarized mode-locked lasers [14, 15,

21–24] have attracted intensive attention for the various applications in optical manipulation of atoms and nanoparticles [25, 26], secure communications [27], control of magnetization [28], and spiral attractor [29]. Therefore, it will be highly desirable to realize the dual-wavelength mode-locked Nd:YAG laser with two orthogonal polarizations.

In this work, we report for the first time on a synchronized self-mode-locked 1061-nm and 1064-nm monolithic Nd:YAG laser at cryogenic temperatures with two orthogonally polarized emissions. The temperature dependent fluorescence spectra for the ${}^4F_{3/2} \rightarrow {}^4I_{11/2}$ transition in the Nd:YAG crystal are explored to find that the emission strengths at 1061 and 1064 nm can reach a comparable level at a temperature near 190 K. We further design a monolithic laser formed by a coated Nd:YAG crystal to explore the output performance for the ${}^4F_{3/2} \rightarrow {}^4I_{11/2}$ transition at the temperature range from 120 K to 290 K. It is observed that the synchronized self-mode-locked 1061-nm and 1064-nm emissions can be successfully realized at the temperature near 190 K and the total output power can be up to 2.5 W at an incident pump power of 5.5 W. The mode-locked pulse width and repetition rate are measured to be 29 ps and 7.75 GHz, respectively. Thanks to the synchronization of the dual-wavelength emissions, the individual mode-locked pulse displays a beat frequency of 670 GHz. On the other hand, we also investigate the polarization characteristics to discover that the laser output comprises two orthogonally polarized components with a central frequency difference of 127 MHz. The central frequency difference between two orthogonal polarizations is experimentally confirmed to come from the external mechanical stress introduced by the copper holder for the laser crystal. It is believed that the present work provides a promising way to generate a series of ultrashort pulses with the sub-terahertz repetition rate with orthogonal polarizations.

2. Experimental setup

The experimental setup for the 1.06- μm self-mode-locked monolithic Nd:YAG laser with two orthogonally polarized emissions at cryogenic temperatures is schematically depicted in Fig. 1. The gain medium was a 1.1 at. % Nd:YAG crystal with a length of 10.63 mm and a transverse aperture of 3 x 3 mm². We employed the laser crystal with coating on both end facets to form a monolithic cavity. The front surface of the monolithic Nd:YAG crystal was high-reflectivity coated at 1060-1070 nm (HR, R > 99.8%) and high-transmittance coated at 808 nm (HT, T > 95%) while the output surface was partially reflection coated at 1060-1070 nm (R = 95%). The laser crystal wrapped with indium foil was mounted in an oxygen-free copper holder and placed in a vacuum chamber. The copper holder was attached to the cold finger of the temperature-controlled cryostat (VPF-100, Janis Research Co.). A calibrated Pt-Au thermocouple was applied on the material surface with a nano-voltmeter (Lake Shore 331) for temperature measurement.

The pump source was a 10-W 808-nm fiber-coupled laser diode with a core diameter of 200 μm and a numerical aperture of 0.16. The pump beam with the diameter of approximately 200 μm was reimaged into the laser crystal through a lens set with a focal length of 50 mm and a coupling efficiency of 90%. The lasing spectral information was monitored by a Fourier optical spectrum analyzer (Advantest Q8347) which is constructed with a Michelson interferometer with a resolution of 0.003 nm. The polarization-resolved mode-locked pulses were detected by two high-speed InGaAs photodetectors with the rise time 35 ps (Electro-optics Technology Inc. ET-3500), whose output signal were sent to a digital oscilloscope (Teledyne LeCroy, Wave Master 820Zi-A) with 20 GHz electrical bandwidth and sampling interval of 25 ps. The pulse width for the mode-locked pulse train was measured with an autocorrelator (APE pulse check, Angewandte Physik & Elektronik GmbH).

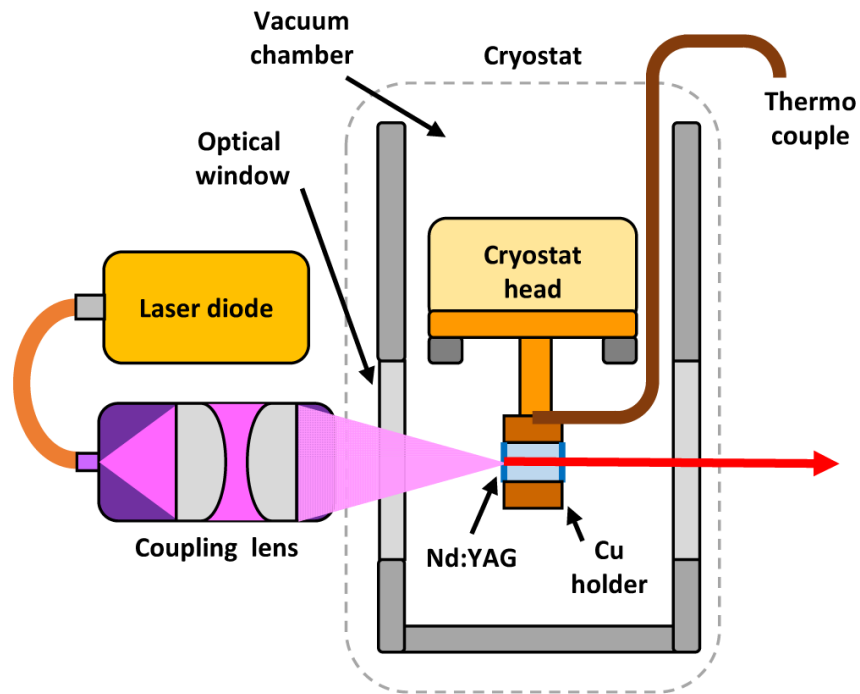


Fig. 1. Experimental setup for the monolithic Nd:YAG laser at cryogenic temperatures.

3. Experimental results

The temperature-dependent fluorescence spectra of the Nd:YAG crystal have been explored in our previous work [17]. Figure 2 shows the fluorescence spectra at particular temperatures of 290 K, 190 K and 120 K. The peak intensities of 1061 and 1064 nm are normalized and thoroughly observed from 90 K to 290 K. The fluorescence intensity at 1061 nm (I_{1061nm}) started to rise with decreasing temperature and reached maximum at the lowest temperature of the system, while the one at 1064 nm (I_{1064nm}) began to fall and split into two apparent peaks. It can be seen clearly that I_{1061nm} became equivalent to I_{1064nm} at approximately 190 K, indicating the feasibility of simultaneous dual-wavelength operation in a cryogenically cooled Nd:YAG laser. Furthermore, the full width at half maximum (FWHM) of two peaks both shrunk gradually through the cooling process, which implies that the number of longitudinal lasing modes has a decreasing tendency. This is fairly beneficial for the self-mode-locked operation thanks to the significant enhancement in the pulse stability [30].

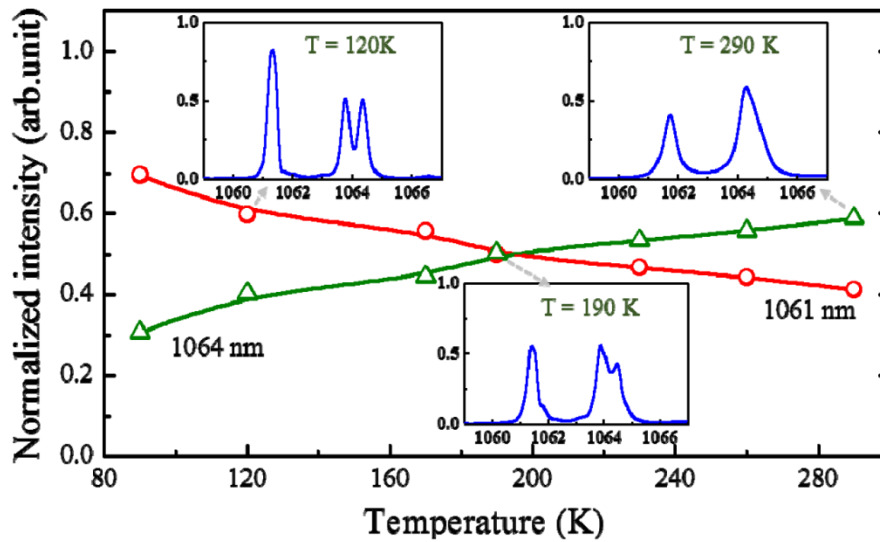


Fig. 2. Normalized intensity of the two dominant peaks at 1061 and 1064 nm with respect to the temperature. The inset: the fluorescence spectra in the range of 1060-1066 nm for temperatures of 120, 190, and 290 K.

In the following, we explored the output performance for the monolithic Nd:YAG laser in a temperature range from 120 K to 290 K. Figure 3 depicts the output power with respect to the incident pump power for the Nd:YAG laser at particular temperatures of 120 K, 150 K, 190 K, 240 K, and 290 K. The overall performance is found to be nearly independent of temperature with the optical-to-optical conversion efficiency of 47%. In contrast, the lasing spectra were found to have significant dependence on temperature. Figure 4 demonstrates the lasing spectra especially near 1061 and 1064 nm at an incident pump power of 5.5 W under the particular temperatures corresponding to Fig. 3. At the room temperature of 290 K, lasing modes appeared only at the wavelength of 1064 nm and 7 longitudinal modes were observed. As the temperature was down to 240 K, the lasing peak started to emerge at 1061 nm and the lasing output at 1064 nm had an obvious blue shift. As the temperature was cooled down to 190 K, simultaneous dual-wavelength operation was observed and the output power for each wavelength reached 1.25 W. For the temperature below 150 K, the lasing output was nearly located at the wavelength of 1061 nm only and the reduction in the number of lasing modes as well as the blue shift was experimentally observed. Overall, the phenomenon discovered in the lasing spectra is in excellent agreement with the prediction observed from the fluorescence spectra.

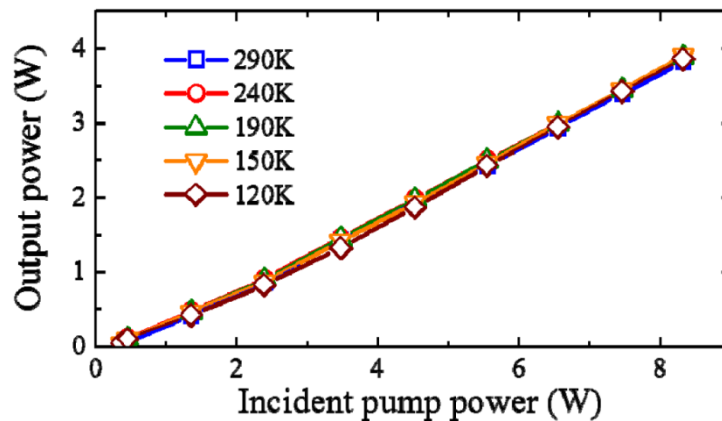


Fig. 3. Output power with respect to the incident pump power for different temperatures of 120, 150, 190, 240, and 290 K.

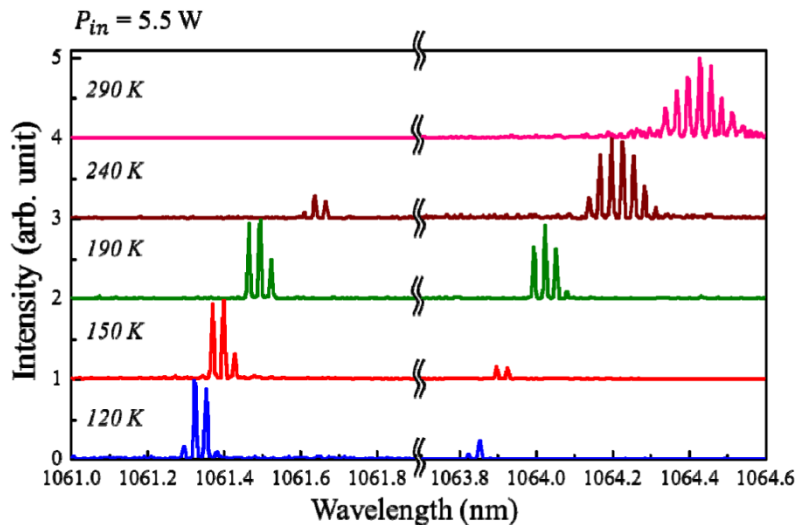


Fig. 4. The lasing spectra at the incident pump power of 5.5 W for different temperatures of 120, 150, 190, 240, and 290 K.

It is noteworthy that the stable CW self-mode-locked operation was experimentally observed at an incident pump power of 5.5 W under 190 K thanks to the adequate amount of longitudinal lasing modes. Figure 5(a) reveals the autocorrelation trace of the synchronized self-mode-locked laser with the delay time of 120 ps. The pulse width is estimated to be 29 ps by assuming the temporal intensity to follow the Gaussian-shaped profile. Furthermore, a strong interference fringe with the modulation depth of 100% is observed in the autocorrelation trace owing to the optical beating between two carrier frequencies of the synchronized mode-locked pulses at 1061 and 1064 nm. The perfect temporal overlapping between the dual-wavelength mode-locked pulses is therefore confirmed. The detailed characteristic of the interference fringe pattern is illustrated in Fig. 5(b) with the delay time of 16 ps. The experimentally measured autocorrelation trace of the optically beat wave could be fitted by means of the cosine-like pulse shape [31]. The optical beat frequency of 670 GHz could be deduced from the pulse period of 1.5 ps and it corresponds well with the central wavelength separation $\Delta\lambda$ of 2.53 nm between the two spectral bands. Note that the modulation depth of the interference fringe pattern would fail to be perfectly 100% at an incident pump power higher than 5.5 W due to the imbalanced intensities of the lasing peak at

1061 nm and 1064 nm. Considering the refractive index of the laser material, the optical length of the cavity was calculated to be approximately 19.35 mm, corresponding to the fundamental pulse repetition rate of 7.75 GHz. Typical oscilloscope trace of the dual-wavelength mode-locked pulse train is illustrated in Fig. 6(a) with the time span of 50 ns. Note that the central wavelengths for each spectral band are located at 1061.49 nm and 1064.02 nm. Besides, the longitudinal mode spacing $\delta\lambda$ of 0.027 nm for both is consistent with the theoretical value deduced from the equation $\delta\lambda = (\lambda^2/c) \cdot \delta f$, where λ is the central wavelength, c is the speed of light, and δf is the free spectral range equal to the pulse repetition rate of the mode-locked laser.

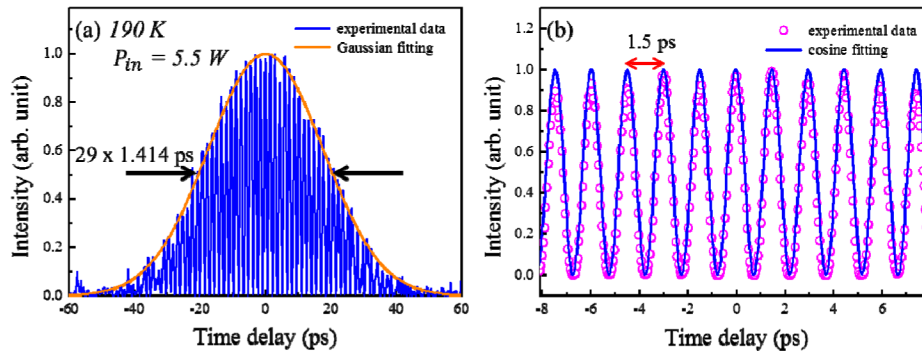


Fig. 5. Autocorrelation traces under 190 K at an incident pump power of 5.5 W with the delay time of (a) 120 ps and (b) 16 ps for the cryogenic monolithic Nd:YAG laser.

Finally, since the orthogonally polarized emissions are verified to exist in the isotropic gain medium, we experimentally observed the induced birefringence in the Nd:YAG laser with cryogenic process. Thanks to the self-mode-locked emission, the birefringence of the isotropic gain medium can be observed by measuring the beat frequency between orthogonally polarized outputs of the mode-locked Nd:YAG laser [15]. More precisely, we employed a polarization beam splitter (PBS) to separate the contribution of polarized component from the laser output. When the PBS was rotated with an angle between orthogonal states, two mode-locked emissions can be coupled and lead to the frequency beating. Since the Fourier optical spectrum analyzer cannot distinguish the relatively slow beating frequency due to the limitation of resolution, we utilized the digital oscilloscope to monitor the temporal behavior of the total output intensity. Figures 6(a) and 6(b) demonstrate the polarization-resolved output intensities at an incident pump power of 1.1 W under 190 K for $\theta = 0^\circ$, $\theta = 90^\circ$, $\theta = 45^\circ$, and $\theta = 135^\circ$, respectively, where θ is the analyzer PBS angle with respect to one polarized component. The pulse trains along the principal polarization directions, corresponding to $\theta = 0^\circ$ and $\theta = 90^\circ$, followed the behavior of typical oscilloscope traces without PBS because the induced birefringence difference was too small to generate different temporal behaviors of self-mode-locked pulses that can be observed by the oscilloscope with limited resolution. On the other hand, the pulse trains of the output intensities along $\theta = 45^\circ$ and $\theta = 135^\circ$ were experimentally found to be modulated by the beat frequency of 127 MHz mainly resulting from the external mechanical stress. Notice that this phenomenon would instantaneously appear once the incident pump power reached the threshold for oscillation and simultaneous dual-wavelength operation was experimentally observed in each principal polarization. The lasing spectra of synchronized self-mode-locked 1061-nm and 1064-nm monolithic Nd:YAG laser with two orthogonally polarized emissions can be briefly schematized in Fig. 7. Two dominant peaks near 1061 and 1064 nm are mainly contributed by the different stark level transitions and the polarization splitting of each dominant peak is introduced by the external stress induced birefringence.

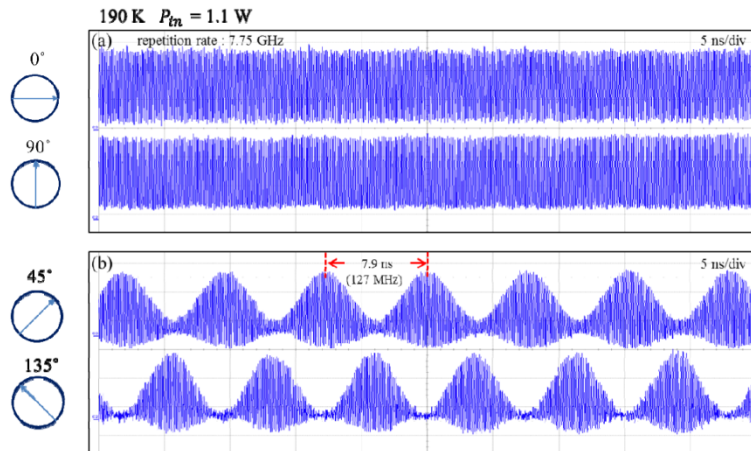


Fig. 6. Temporal traces of the polarization-resolved output intensities under 190 K at an incident pump power of 1.1 W for (a) $\theta = 0^\circ$ and $\theta = 90^\circ$, (b) $\theta = 45^\circ$ and $\theta = 135^\circ$.

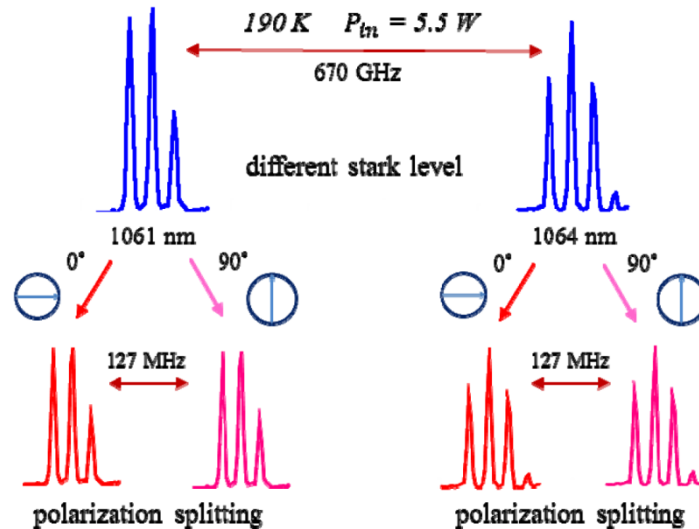


Fig. 7. Schematic diagram of the lasing spectra at 1061 and 1064 nm for the monolithic Nd:YAG laser under 190 K at an incident pump power of 5.5 W.

The relationship between the beat frequency and temperature was further investigated as shown in Fig. 8. At an incident pump power of 1.1 W, the beat frequency was found to increase from 8.8 MHz to 199.0 MHz for the temperature from 290 K to 120 K, indicating an increasingly stronger external stress was put on the laser crystal during the cooling process. This phenomenon can be well explained by the shrinking volume with decreasing temperature and comparison of thermal expansion coefficient, as the change in volume follows the approximated relation $\Delta V = 3\alpha V_i \Delta T$, where α is the thermal expansion coefficient, V_i is the initial volume, and ΔT is the change in temperature. Since copper has the thermal expansion coefficient approximately 3 times larger than YAG crystal under the temperature range from 120 K to 290 K [32, 33], the laser crystal would thus be compressed tightly by the copper holder with decreasing temperature. It is worthwhile to mention that the polarization splitting phenomenon exists in either single-wavelength emission or dual-wavelength emissions.

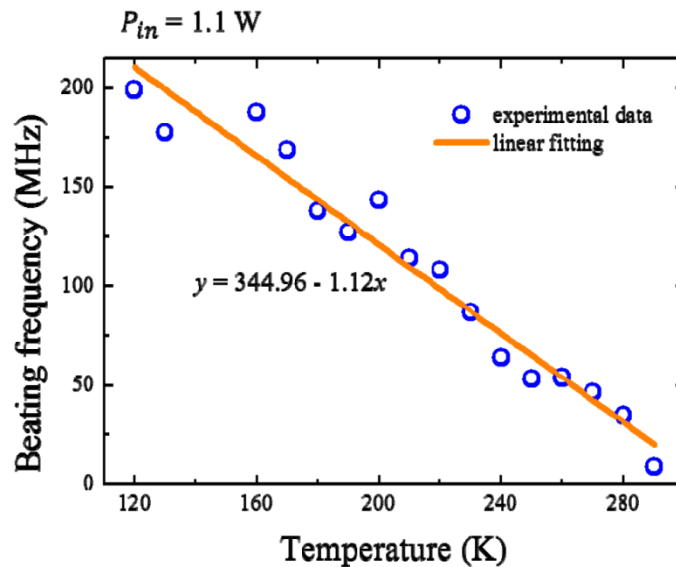


Fig. 8. Beat frequency of the self-mode-locked monolithic Nd:YAG laser measured as a function of temperature at an incident pump power of 1.1 W.

4. Conclusion

In summary, we have demonstrated a synchronized self-mode-locked 1061-nm and 1064-nm monolithic Nd:YAG laser at cryogenic temperatures with two orthogonally polarized emissions for the first time. At an incident pump power of 5.5 W, the total output power of 2.5 W has been generated for the balanced emissions at 1061 and 1064 nm under 190 K with the mode-locked pulse width of 29 ps and repetition rate of 7.75 GHz. Experimental results further reveal that the excellent synchronization between the dual-comb pulses leads to the generation of ultrashort beat signal with repetition rate of 670 GHz. Moreover, it is observed that the laser output consists of two orthogonally polarized mode-locked components with a central frequency difference of 127 MHz. The beating frequency between two orthogonal polarizations results from the external mechanical stress induced birefringence introduced by the copper holder. It is verified that the decrease in temperature would contribute to an increasingly stronger stress intensifying the beating phenomenon. This work is expected to offer a promising method for generating a series of ultrashort pulses with the sub-terahertz repetition rate with orthogonal polarizations.

Funding

Ministry of Science and Technology of Taiwan (MOST-103-2112-M-009-016-MY3).